IJE TRANSACTIONS C: Aspects Vol. 33, No. 3, (March 2020) 668-675

International Journal of Engineering

Journal Homepage: www.ije.ir

A Novel Intelligent Fault Diagnosis Approach for Critical Rotating Machinery in the Time-frequency Domain

B. Attaran, A. Ghanbarzadeh*, S. Moradi

Mechanical Engineering Department, Shahid Chamran University of Ahvaz, Iran

P A P E R I N F O

Paper history:
Received 27 February 2019
Received in revised form 08 November 2019
Accepted 05 March 2020

Keywords:
Fast Kurtogram
Bearing Fault Detection
Statistical Features
Time-frequency Domain

A B S T R A C T

The rotating machinery is a common class of machinery in the industry. The root cause of faults in the rotating machinery is often faulty rolling element bearings. This paper presents a novel technique using artificial neural network learning for automated diagnosis of localized faults in rolling element bearings. The inputs of this technique are a number of features (harmmean and median), which are extracted from the vibration signals of the test data. Effectiveness and novelty of this proposed method are illustrated by using the experimentally obtained the bearing vibration data based on laboratory application. In this research, based on the fast kurtogram method in the time-frequency domain, a technique for the first time is presented using other types of statistical features instead of the kurtosis. For this study, the problem of four classes for bearing fault detection is studied using various statistical features. This study is conducted in four stages. At first, the stability of each feature for each fault mode is investigated, then resistance to load change as well as failure growth is studied. At the end, the resolution and fault detection for each feature using the comparison with a determined pattern and the coherence rate is calculated. From the above results, the best feature that is both resistant and repeatable to different variations, as well as the suitable accuracy of detection and resolution, is selected and with comparing to the kurtosis feature, it is found that this feature is not in a good condition in compared with other statistical features such as harmmean and median. The results show that the accuracy of the proposed approach is 100% by using the proposed neural network, even though it uses only two features.

***doi**: 10.5829/ije.2020.33.04a.18*

1. INTRODUCTION

The desire and need for precision detection capabilities and precautionary predictions have long been equivalent to human use of complex and expensive machines. Efforts to develop and implement varying degrees of detection and anticipation capabilities have a long history. Exploiting rotary machines is one of the major challenges in maintenance and repair. Intelligent maintenance and repair, as well as diagnosis and prediction of deficiencies, are essential for the oil, gas, refinery, petrochemical, transportation, aerospace, military and commercial vessels, automation and other industries. Diagnosing and anticipating defects is one of the challenging issues of the health management system and the anticipation of modern defects. Reduces the cost of support and operation, as well as the total cost of ownership over the life cycle, and improves the level of safety of many types of machinery and complex systems. The evolution of fault diagnostic monitoring systems for rotating equipment and other complex systems helps to realize that it is possible to identify predictive defects desirable and technically possible. The most important challenge is addressing the signal of roller bearing defects. Bearing defects are produced in the form of blows caused by passing roll elements on the surface of the failure. Identifying and monitoring these flaws is difficult, especially in the early stages of the defect, which is a very small failure and is easily covered with other components. Undoubtedly, all defect prediction techniques need to be further developed to better adapt to the characteristics of nonlinear systems

*Corresponding Author Email: *Ghanbarzadeh.A@scu.ac.ir* (A. Ghanbarzadeh)

Please cite this article as: B. Attaran, A. Ghanbarzadeh, S. Morad, A Novel Intelligent Fault Diagnosis Approach for Critical Rotating Machinery in the Time-frequency Domain, International Journal of Engineering (IJE), IJE TRANSACTIONS C: Aspects Vol. 33, No. 3, (March 2020) 668-675

so that they can be used in real-world conditions. Yang et al. [1] used a new time-frequency domain called base track that was recently created. In fact, they used the application of this new method to extract the characteristics of the faulty roller bearing signals with internal and external cannon failures. They showed that the failure characteristics of the base tracking technique create a better resolution in the time-frequency domain. Liang and Bochalooi[2] proposed an energy operator method for frequency and domain division; they showed that the Tiger energy operator is suitable for extracting the frequency modulation and the amplitude of the vibrational signals of mechanical systems. Due to the continuity of frequency modulation information in this method, there is no need for multiple steps to remove unwanted components. So that the range of diamonds inherently in the energy operator can determine the failure frequency from the energy spectrum of the energy conversion. Suu et al. [3] presented a new compound-based Morellet wavelet filtering method that improves self-dependency. Initially, in order to eliminate the frequency of interference vibrations, the vibration signal is filtered by the midpoint filter specified by the Morellet wavelet. Also, the parameters associated with the Morellet wavelet, including the central frequency and bandwidth, are optimized by the genetic algorithm, whose target function is the minimization criterion for Shannon entropy. Doo et al. [4] introduced a new intelligent method for diagnosing rotary machines based on intrinsic mode decomposition, dimensional parameters, decomposition table, law inference algorithm called second editing tutorial for modified modules examples and modified strategy for implementing the presentation law. The EMD method for preprocessing vibrating signals is used to accurately derive the characteristics of the failure. Then, the non-dimensional parameters extracted from the decomposed signals in the time domain and the Enolop spectrum in the frequency domain are obtained for the decomposition table.

Lee et al. [5] presented a new classifier based on the lattice framework for the classification of the friction grid for the problem of detecting bearing defects. This method does not need to determine any parameters and converges at a high speed with a small number of inference law. To illustrate the results, they used five datasets, and ultimately demonstrated their efficiency and accuracy compared to the same method of fuzzy network argumentation and other neural networks.

Wang et al. [6] presented the advanced Kurtogram method for detecting roller bearing defects. The decoder is based on the elongation of the time signals that are filtered by the Fourier transform. Also, the transformation of the wavelet packet is also used as a substitute for the Fourier transform of the short time to analyze the signal in this method. This method helps in determining the location of frequency amplification bands for further modulation. Finally, the frequency characteristics of the ANOLOP signal are used to determine the type of bearing failure. Zhou and Chen [7] provided an intelligent diagnostic method based on the least squares of the back propagation machine optimized by the modified particle optimization method. First, the initial vibration signals are decomposed into several intrinsic mode functions, which is done by the EMD method and the energy attribute values extracted based on the energy-entropy of the IMF. Finally, the energy indicators extracted as breakdown property vectors, the IPSO-LSSVM classifier inputs, are used to identify the different failure patterns.

Albuagbi and Trondaphilova [8] presented a method for identifying roller bearing defects. Their method consists of two main steps. Pretreatment of signals, based on several signal analysis algorithms and defect detection, which uses the pattern recognition process. The first step is, in fact, linear time constant based on automated modeling of regression. In the pre-purification step, the spectral analysis method is used to remove noise from the signal. Baraldi and colleagues [9] presented a method to identify the beginning of a failure, to detect defective bearings in the system, to classify the type of failure, and to determine the severity of the failure. Their fault diagnosis is based on the hierarchical structure associated with the classification of the nearest neighbor K. Feature selection The vibration signals for the input of the fault diagnostic system are based on the packaging method based on the multi-objective optimization integrated with the binary differential algorithm and the KNN classifier.

Vakharia et al. [10] presented an algorithm for detecting various bearing defects of measured vibrational signals. Characteristics such as elongation, squaring, mean, root mean squares, or more complex features such as Shannon entropy from the time domain, frequency domain, and discrete wavelet transform are calculated. Feature rating methods such as Qi square and Assist-F method are used to select the best feature.

Singh et al [11] presented an algorithm based on a flexible, logically wavelet transform. Their method in frequency segmentation is flexible to produce a number of filters with a variety of bandwidths. The optimal filter selection, which is completely overlapping with bearing defects in the excited region, is performed based on the maximum amount of shock detection provided by the "self-bonding elongation of the intermediate energy" function.

2. KURTOGRAM

Despite the benefits of wavelet transformation, challenges include choosing the right mother-wavelet

from a variety of examples, as well as high computational costs, especially for smaller scale levels. These challenges have suggested different ways to improve the wavelet transform or different ways to select the appropriate maternal wavelet. Some of these improvements are mentioned in previous studies. On the other hand, these challenges in the transformation of the wavelet have led to the emergence of other methods, such as the spectral kurtosis and Kurtogram.

The Kurtogram method is based on the Spectral Kurtosis, which is a high-order statistical method. In 1983, the first use of the frequency spectrum was carried out by Dewey. In the following years, this method quickly progressed and improved for a variety of applications. Then, Anthony proposed in 2004 the elongation based on the Vold-Cramer decomposition, which described each non-terminal signal as the output of a variable-time linear system.

The ensemble machine learning techniques were demonstrated for the detection of different AFB faults [12]. Initially, statistical features were extracted from temporal vibration signals and were collected using experimental test rig for different input parameters like load, speed and bearing conditions. Heidari [13] has proposed a reduct construction method based on discernibility matrix simplification. The method worked with the genetic algorithm. To identify potential problems and prevent complete failure of bearings, a new method based on rule-based classifier ensemble was presented.

Li et al. [14] focused on the problem of accurate Fault Characteristic Frequency (FCF) estimation of the rolling bearing. Teager-Kaiser Energy Operator (TKEO) demodulation has been applied widely to rolling bearing fault detection. FCF could be extracted from vibration signals, which was pre-treatment by TKEO demodulation method.

In the further development of the Kurtogram in 2018, Musharrafzadeh and Fassana [15] showed that, despite the capabilities of the QuickTech method. Therefore, the autogram method is introduced. Which is largely similar to the same method, with the difference that the calculation of the elongation based on the self-correlation of the signal obtained from the Envelop square in the frequency bands, which partially succeeded in increasing the accuracy of the failure detection and lowering the computational cost [16].

So according to the above, new methods such as spectral kurtosis, fast Kurtogram, autogram have been developed to replace the wavelet. All of these methods are based on the statistic feature of the kurtosis. In this study, a new time-frequency domain was introduced, and other commonly used statistical features are used instead of the kurtosis feature. The proposed process is as follows:

1. Design of low pass and high pass filters for binary decomposition, as well as the design of low pass, band-pass and high pass filters for ternary of signal analysis.
2. The signal once decomposed into binary and ternary, then each section of the binary decomposition is again degraded the again binary and ternary, and the same trend continues for higher decomposition levels.
3. Calculate common features for each section obtained from the previous step for comparison
4. Choosing the proper features

For this purpose, the feature should be chosen so that the time-frequency domain derives from the following conditions :

Firstly, the time-frequency domain must be robust and repeatable for failure with specified type and severity. That is, different measured signals for a failure type provide the same time-frequency domain .

Secondly, the time-frequency domain for each fault mode must be resilient and repeatable to changes in conditions such as load change. That is, with different loads, the same time-frequency domain is achieved .

Thirdly, The time-frequency domain for each failure should be robust and repeatable against the growth failure. In other words, in the case of breakdowns with different depths, but of the same type, the time-frequency domain presents a relatively similar behavior .

Fourth, the ability to detect and differentiate the time-frequency domain of each feature is appropriate for various failures. Below are the statistical features that are being studied in this study:

Data samples can have thousands (even millions) of values. Descriptive statistics can summarize these data into a few numbers that contain most of the relevant information. The following statistical parameters are used to detect incipient bearing damage: root mean square, interquartile range, skewness, mean, geometric mean, harmonic mean, mean excluding outliers, largest element, smallest element, most frequent value, standard deviation, variance, median, range, sum, trapezpidal integration, mean absolute deviation, moment and percentiles. where X_i (i=1, …, N) is the amplitude at sampling point i and N is the number of sampling points. μ is the mean of X, σ is the standard deviation of X, and E(.) represents the mathematical expectation.

3. EXPERIMENTAL SETUP

The vibration data used in this study were obtained from the dataset of the rolling element bearings under different operating loads and bearing conditions according to Table 1. The ball bearings are installed in a motor-driven mechanical system. An accelerometer, with a frequency range of 20-20 kHz is mounted on the motor housing at the drive end of the motor to acquire the vibration signals from the bearing. The data

collection system consists of a data recorder with a sampling frequency of 12 kHz per channel. The defect size (diameter, depth) of the three faults was the same, 0.007", 0.014", 0.021" and 0.028". Each bearing was tested under four different loads, (e.g. 0, 1, 2, and 3 hp corresponding to 0, 0.736, 1.491, and 2.237 kW). The motor speed during the experimental tests was 1720-1797 r/min. The bearing dataset was obtained from the experimental system under the four different operating conditions: (1) normal condition; (2) inner race fault; (3) ball fault; and (4) outer race fault.

In order to develop a robust fault diagnosis model that is able to identify the existence of different faults under varying load conditions, and to evaluate the proposed methods, this fault diagnosis problem is set as a four-class classification problem.

4. RESULTS AND DISCUSSION

4. 1. First Stage First, the resistance of the time-frequency domain of each figure must be checked for any specific failure. For this purpose, ten raw signals are considered for each mode, then using one of the introduced features, the time-frequency domain is calculated and the resulting matrix is normalized. Finally, the standard deviation of ten time-frequency domains is calculated relative to each other. The lower standard deviation leads to be more robust and repeatable of the time-frequency domain.

In Table 2, anyone whose total rank is less than that, the time-frequency domain resulting from it is more resistant and more repeatable. As you can see, the feature of kurtosis in this comparison is not good.

4. 2. Second Stage At this stage, the resistance of the time-frequency domain to the change in load must be checked. For this purpose, for each of the three types of failure, four magnitudes of the load are considered, and after using the time-frequency domain statistical features, and then, the standard deviation of the four time-frequency domains is calculated. Eventually, any feature whose total deviation is less than normal will naturally be more resistant to detecting according to Table 3.

TABLE 1. Dataset of Case Western Reserve University

Fault Diameter	Motor Load (HP)	Motor Speed (rpm)	Normal	Inner Race	Ball	Outer Race
Normal	0	1797	C1	*	*	*
	1	1772		*	*	*
	2	1750		*	*	*
	3	1730		*	*	*
0.007"	0	1797	*	C2	C3	C4
	1	1772	*			
	2	1750	*			
	3	1730	*			
0.014"	0	1797	*			
	1	1772	*			
	2	1750	*			
	3	1730	*			
0.021"	0	1797	*			
	1	1772	*			
	2	1750	*			
	3	1730	*			
0.028"	0	1797	*			*
	1	1772	*			*
	2	1750	*			*
	3	1730	*			*

TABLE 2. The stability of each feature for each fault mode

No.	Feature	Inner race	Rank 1	Ball fault	Rank 2	Outer race	Rank 3
1	Kurtosis	1.039	18	2.242	19	0.722	16
2	Rms	0.134	8	0.103	3	0.074	4
3	IQR	0.299	13	0.289	11	0.398	12
4	Skewness	1.401	20	2.382	20	0.911	19
5	Mean	0.194	11	0.109	5	0.141	10
6	Geomean	0.350	15	0.253	10	0.768	17
7	Harmmean	0.993	17	0.922	16	0.524	13
8	Trimmean	0.257	12	0.136	6	0.620	14
9	Max	0.134	9	0.465	14	0.118	8
10	Min	0.641	16	0.937	17	0.896	18
11	Mode	1.363	19	1.295	18	1.128	20
12	Std	0.090	5	0.187	9	0.090	5
13	Var	0.049	3	0.105	4	0.036	3
14	Median	0.315	14	0.357	12	0.637	15
15	Range	0.144	10	0.467	15	0.114	7
16	Sum	0.005	1	0.008	1	0.006	1
17	Trapz	0.005	2	0.008	2	0.006	2
18	Mad	0.096	6	0.172	8	0.120	9
19	Moment	0.084	4	0.162	7	0.101	6
20	Prctile	0.131	7	0.381	13	0.146	11

TABLE 3. Resistance of each feature to load change

No	Feature	Inner race	Rank 1	Ball fault	Rank 2	Outer race	Rank 3
1	Kurtosis	1.092	19	2.636	19	0.450	12
2	Rms	0.342	9	0.218	9	0.144	6
3	IQR	0.405	12	0.234	12	0.642	15
4	skewness	0.762	18	2.653	20	0.515	13
5	Mean	0.378	11	0.227	11	0.238	11
6	Geomean	0.594	15	0.236	13	1.968	20
7	harmmean	0.561	14	1.163	16	1.310	19
8	trimmean	0.511	13	0.215	8	0.672	16
9	Max	0.339	7	0.299	14	0.151	8
10	Min	0.599	16	1.761	18	0.555	14
11	Mode	1.193	20	1.509	17	0.918	17
12	Std	0.279	5	0.171	5	0.103	4
13	Var	0.223	4	0.102	3	0.060	3
14	Median	0.636	17	0.203	7	0.956	18
15	Range	0.342	10	0.301	15	0.173	9
16	Sum	0.019	2	0.015	1	0.012	2
17	Trapz	0.019	1	0.015	2	0.012	1
18	Mad	0.341	8	0.178	6	0.187	10
19	Moment	0.332	6	0.168	4	0.147	7
20	Prctile	0.213	3	0.222	10	0.112	5

TABLE 4. Resistance of each feature to failure growth

No	Feature	Inner race	Rank1	Ball fault	Rank 2	Outer race	rank 3
1	Kurtosis	3.614	20	3.323	20	5.262	19
2	Rms	0.625	10	0.398	8	0.464	5
3	IQR	1.120	13	0.415	10	3.880	18
4	Skewness	3.522	19	2.779	19	5.585	20
5	Mean	0.798	11	0.607	12	0.564	6
6	Geomean	1.451	16	1.068	15	3.591	16
7	harmmean	1.249	15	1.147	17	3.230	15
8	trimmean	1.020	12	0.834	13	2.216	14
9	Max	0.387	4	0.317	4	0.256	3
10	Min	1.156	14	1.444	18	0.569	7
11	Mode	1.505	17	1.100	16	1.838	13
12	Std	0.541	6	0.415	11	1.090	10
13	Var	0.425	5	0.318	6	0.754	9
14	Median	1.542	18	1.027	14	3.867	17
15	Range	0.377	3	0.316	3	0.256	4
16	Sum	0.067	2	0.052	2	0.076	2
17	Trapz	0.067	1	0.052	1	0.076	1
18	Mad	0.555	7	0.379	7	1.518	12
19	Moment	0.576	8	0.400	9	1.374	11
20	Prctile	0.582	9	0.317	5	0.722	8

4. 3. Third Stage In this section, it is necessary to select a feature that the time-frequency domain resulting from it will not fail against the growth of the failure. For this purpose, for each failure, four growth stages are considered and ultimately the standard deviation of the four time-frequency domains obtained for each feature is calculated and the results are presented in Table 4.

4. 4. Fourth Stage In this phase, the decomposability of the failures is investigated using the time-frequency domain derived from different statistical features. For this purpose, for each failure, a time-frequency domain is already considered as a pattern, and then for each new signal, it receives the corresponding time-frequency domain and compares with the four previous patterns. Coherence has been used to calculate the similarity of each time-frequency domain with patterns. The coherence number is closer to one, the two are more similar, and it approaches zero, they are more different.

Tables 5a and 5b have two parts; first, each breakdown is compared to its own pattern, the sum of which is the true column. Then, the similarity of each failure with the other failure patterns is compared, and their sum is also the false column. Now the feature is appropriate to have a greater true value and simultaneously the false value is low. For this review, Tables 5a and 5b are depicted in Figure 1.

In Figure 1, the horizontal direction is reversed for a better look. Now the feature should be selected to have a more True value and less False value, or closer to the origin of Figure 1, so the two harmmean and median features are the most appropriate ones.

Figure 2 is displayed using the kurtosis feature according to literature [17, 18]. As you can see, the first and third classes, as well as the second and fourth, are relatively similar. Then, this feature has less resistance and repeatability in contrast to the change in load and the growth of the failure and even in a certain fault.

Figure 3 is derived using the harmmean feature. As you can see, all four classes are different, and the time-frequency domains of each fault with its failure pattern match entirely. In the tables of the first stage to the third stage can be perceived as a good repeatability status against load change and deterioration.

TABLE 5a. Comparison with a pattern and the coherence rate

No	Feature	1,1	2,2	3,3	4,4	True	1,2	1,3
1	kurtosis	0.49	0.73	0.40	0.84	2.45	0.15	0.37
2	Rms	1.00	1.00	0.98	1.00	3.98	0.23	0.27
3	IQR	0.99	0.94	0.90	0.99	3.81	0.22	0.27
4	skewness	0.44	0.56	0.41	0.54	1.95	0.28	0.35
5	Mean	1.00	1.00	0.98	1.00	3.98	0.24	0.27
6	geomean	1.00	0.99	0.97	0.99	3.95	0.24	0.26
7	harmmean	0.98	0.92	0.90	0.94	3.74	0.23	0.23
8	trimmean	1.00	0.99	0.98	1.00	3.97	0.24	0.26
9	Max	0.98	0.98	0.95	1.00	3.91	0.30	0.29
10	Min	0.85	0.64	0.46	0.69	2.64	0.43	0.32
11	Mode	0.77	0.60	0.72	0.66	2.74	0.36	0.22
12	Std	0.99	0.99	0.97	1.00	3.95	0.24	0.28
13	Var	1.00	1.00	0.99	1.00	3.98	0.35	0.39
14	median	1.00	0.98	0.98	0.97	3.92	0.23	0.27
15	Range	0.98	0.98	0.95	0.99	3.90	0.30	0.29
16	Sum	1.00	1.00	1.00	1.00	4.00	0.66	0.62
17	Trapz	1.00	1.00	1.00	1.00	4.00	0.66	0.62
18	Mad	0.99	0.98	0.97	1.00	3.94	0.23	0.28
19	moment	0.99	0.99	0.97	1.00	3.95	0.23	0.29
20	Prctile	0.99	0.98	0.96	1.00	3.93	0.26	0.28

TABLE 5b. Comparison with a pattern and the coherence rate

1,4	2,1	2,3	2,4	3,1	3,2	3,4	4,1	4,2	4,3	False
0.07	0.18	0.19	0.39	0.38	0.15	0.10	0.10	0.39	0.12	2.57
0.27	0.23	0.51	0.60	0.26	0.54	0.83	0.27	0.62	0.80	5.44
0.25	0.22	0.47	0.46	0.25	0.49	0.75	0.26	0.44	0.70	4.78
0.29	0.26	0.30	0.26	0.33	0.30	0.26	0.23	0.30	0.28	3.44
0.26	0.23	0.48	0.56	0.26	0.51	0.81	0.26	0.57	0.79	5.25
0.25	0.23	0.44	0.50	0.26	0.47	0.72	0.24	0.52	0.69	4.81
0.22	0.23	0.38	0.41	0.23	0.41	0.51	0.22	0.42	0.47	3.96
0.25	0.23	0.45	0.52	0.26	0.48	0.79	0.25	0.52	0.77	5.02
0.33	0.28	0.62	0.79	0.28	0.67	0.81	0.32	0.79	0.79	6.27
0.32	0.45	0.36	0.44	0.33	0.37	0.35	0.39	0.56	0.34	4.66
0.27	0.42	0.20	0.40	0.07	0.06	0.16	0.38	0.56	0.15	3.24
0.29	0.23	0.55	0.64	0.27	0.59	0.78	0.29	0.67	0.76	5.59
0.35	0.34	0.67	0.70	0.38	0.72	0.83	0.34	0.73	0.81	6.59
0.24	0.23	0.43	0.46	0.25	0.45	0.67	0.23	0.48	0.69	4.64
0.34	0.28	0.63	0.79	0.29	0.67	0.81	0.33	0.79	0.80	6.32
0.59	0.67	0.96	0.93	0.62	0.96	0.98	0.60	0.94	0.98	9.50
0.59	0.67	0.96	0.93	0.62	0.96	0.98	0.60	0.94	0.98	9.51
0.28	0.23	0.52	0.59	0.26	0.56	0.78	0.28	0.61	0.76	5.38
0.29	0.23	0.53	0.61	0.27	0.57	0.78	0.28	0.63	0.76	5.47
0.31	0.24	0.56	0.72	0.27	0.61	0.78	0.30	0.75	0.76	5.83

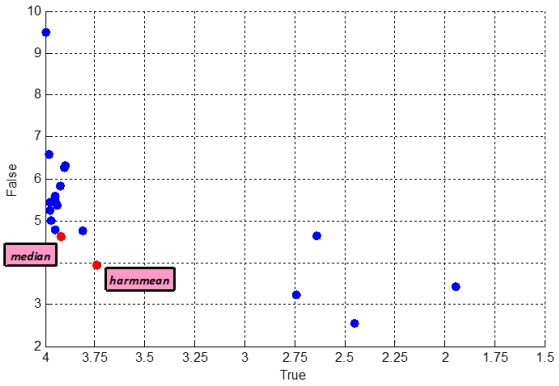

Figure 1. Coherence rate of each feature

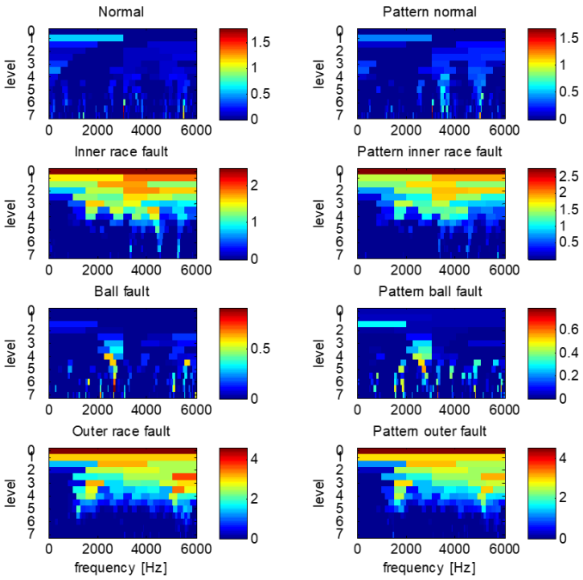

Figure 2. The Fast Kurtogram using kurtosis feature

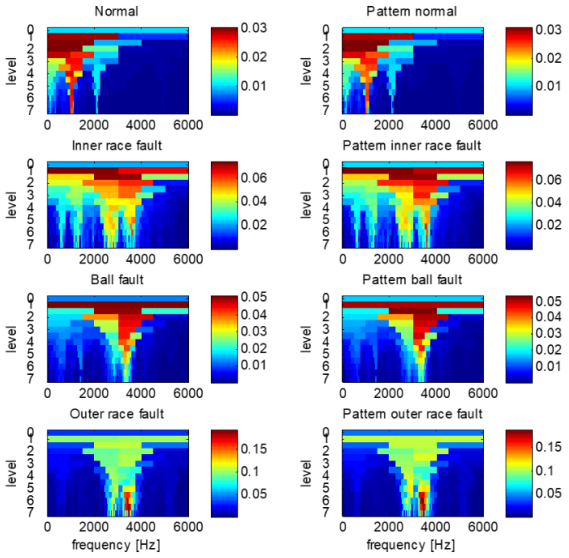

Figure 3. The Fast Kurtogram using harmmean feature

5. THE PROPOSED METHOD FOR DIAGNOSTICS

The characteristics of proposed artificial neural network for diagnostics task are described as following:

1. Data Division: Random (dividerand)
2. Training: Scaled Conjugate Gradient (trainscg)
3. Performance: Mean Squared Error (mse)
4. The best features for diagnostics: Kurtogram + harmmean

This optimal neural network is shown in Figure 4. The mean squared error is plotted according to Figure 5.

The plot of error histogram with 20 bins and the gradient and validation checks at epoch 72 are demonstrated in Figure 6. The results of fault diagnosis is depicted in Figure 7.

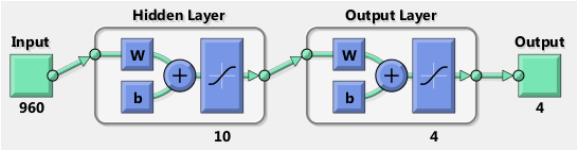

Figure 4. The structure of ANN for proposed method

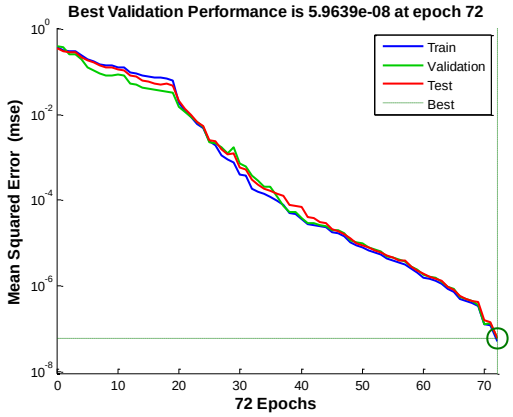

Figure 5. Plot of mean squared error

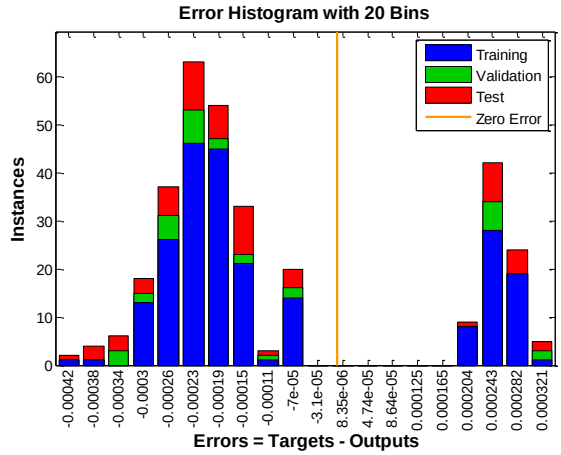

Figure 6. Plot of error histogram with 20 bins

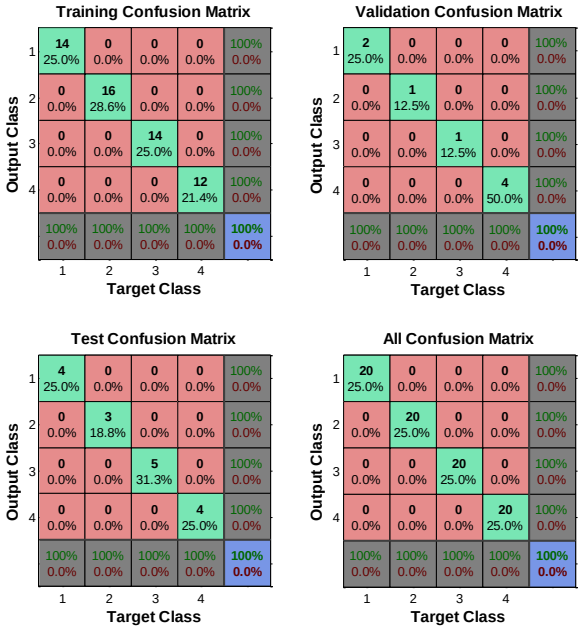

Figure 7. Plot of training, test and validation confusion matrix

6. CONCLUSION

In this paper, based on the technique of fast kurtogram, the novel technique was introduced on other types of statistical features instead of the kurtosis for the first time. To this purpose, we examined the issue of four classes of bearing fault detection by using 20 different statistical features. This study was conducted in four stages. At first, the stability of each feature was checked for each failure. Then resistance to load change and failure growth was studied. At the end, the resolution and fault detection for each feature was calculated. From the above results, the best feature, which was both resistant and repeatable to different variations, as well as accurate detection and resolution was selected, and it was found that the kurtosis is not well-positioned in comparison with other statistical attributes such as harmmean and median. In this research that was done based on kurtogram method, in fact instead of using kurtosis feature, other statistical features were utilized. In future work, it can be implemented that instead of using time signal in the frequency bounds, at the first the signal processing methods will be applied, then kurtosis feature will be calculated from signal processing, and the result will be compared with the kurtogram method. In this work, we have investigated the problem of automatic bearing fault diagnosis using machine learning methods based on artificial neural network. These methods consist of feature extraction, feature selection, and classification. eventually only two features with better performance were chosen as the input features to the classifier and have been verified by the machinery fault simulator test rig.

7. REFERENCES

1. Yang, H., Mathew, J. and Ma, L., "Fault diagnosis of rolling element bearings using basis pursuit", ***Mechanical Systems and Signal Processing***, Vol. 19, No. 2, (2005), 341-356.
2. Liang, M. and Soltani Bozchalooi, I., "An energy operator approach to joint application of amplitude and frequency-demodulations for bearing fault detection", ***Mechanical Systems and Signal Processing***, Vol. 24, No. 5, (2010), 1473-1494.
3. Su, W., Wang, F., Zhu, H., Zhang, Z. and Guo, Z., "Rolling element bearing faults diagnosis based on optimal morlet wavelet filter and autocorrelation enhancement", ***Mechanical Systems and Signal Processing***, Vol. 24, No. 5, (2010), 1458-1472.
4. Dou, D., Yang, J., Liu, J. and Zhao, Y., "A rule-based intelligent method for fault diagnosis of rotating machinery", ***Knowledge-Based Systems***, Vol. 36, (2012), 1-8.
5. Li, B., Liu, P.-y., Hu, R.-x., Mi, S.-s. and Fu, J.-p., "Fuzzy lattice classifier and its application to bearing fault diagnosis", ***Applied Soft Computing***, Vol. 12, No. 6, (2012), 1708-1719.
6. Wang, D., Tse, P.W. and Tsui, K.L., "An enhanced kurtogram method for fault diagnosis of rolling element bearings", ***Mechanical Systems and Signal Processing***, Vol. 35, No. 1, (2013), 176-199.
7. Xu, H. and Chen, G., "An intelligent fault identification method of rolling bearings based on lssvm optimized by improved pso", ***Mechanical Systems and Signal Processing***, Vol. 35, No. 1, (2013), 167-175.
8. Al-Bugharbee, H. and Trendafilova, I., "A fault diagnosis methodology for rolling element bearings based on advanced signal pretreatment and autoregressive modelling", ***Journal of Sound and Vibration***, Vol. 369, (2016), 246-265.
9. Baraldi, P., Cannarile, F., Di Maio, F. and Zio, E., "Hierarchical k-nearest neighbours classification and binary differential evolution for fault diagnostics of automotive bearings operating under variable conditions", ***Engineering Applications of Artificial Intelligence***, Vol. 56, (2016), 1-13.
10. Vakharia, V., Gupta, V.K. and Kankar, P.K., "Bearing fault diagnosis using feature ranking methods and fault identification algorithms", ***Procedia Engineering***, Vol. 144, (2016), 343-350.
11. Singh, J., Darpe, A.K. and Singh, S.P., "Rolling element bearing fault diagnosis based on over-complete rational dilation wavelet transform and auto-correlation of analytic energy operator", ***Mechanical Systems and Signal Processing***, Vol. 100, (2018), 662-693.
12. Patil, S. and Phalle, V., "Fault detection of anti-friction bearing using ensemble machine learning methods", ***International Journal of Engineering***, ***Transaction B: Applications***, Vol. 31, No. 11, (2018), 1972-1981.
13. Heidari, M., "Fault detection of bearings using a rule-based classifier ensemble and genetic algorithm", ***International Journal of Engineering, Transactions A: Basics***, Vol. 30, No. 4, (2017), 604-609.
14. Li, X., Han, L., Xu, H., Yang, Y. and Xiao, H., "Rolling bearing fault analysis by interpolating windowed dft algorithm", ***International Journal of Engineering, Transactions A: Basics***, Vol. 32, (2019), 121-126.
15. Moshrefzadeh, A. and Fasana, A., "The autogram: An effective approach for selecting the optimal demodulation band in rolling element bearings diagnosis", ***Mechanical Systems and Signal Processing***, Vol. 105, (2018), 294-318.
16. Antoni, J., "The spectral kurtosis of nonstationary signals: Formalisation, some properties, and application", in 2004 12th European Signal Processing Conference., (2004), 1167-1170.
17. Antoni, J. and Randall, R.B., "The spectral kurtosis: Application to the vibratory surveillance and diagnostics of rotating machines", ***Mechanical Systems and Signal Processing***, Vol. 20, No. 2, (2006), 308-331.
18. Antoni, J., "Fast computation of the kurtogram for the detection of transient faults", ***Mechanical Systems and Signal Processing***, Vol. 21, No. 1, (2007), 108-124.

Persian Abstract

چکیده

در این مقاله بر مبنای روش کرتوگرام سریع در حوزه زمان فرکانس، تکنیکی برای اولین بار با استفاده از دیگر انواع فیچرهای آماری بجای فیچر کرتوسیس ارائه شده است. برای این مطالعه مسئله چهار کلاسه‌ی تشخیص عیب بیرینگ را با استفاده از فیچرهای آماری مختلف مورد بررسی قرار گرفته است. این مطالعه در چهار مرحله انجام شده است. ابتدا مقاوم بودن هر فیچر برای هر نوع خرابی بررسی شده، سپس مقاوم بودن در برابر تغییر بار و همچنین رشد خرابی مورد مطالعه قرار گرفته است. در انتها میزان تفکیک‌پذیری و تشخیص خرابی برای هر فیچر با استفاده از مقایسه با یک الگو از قبل مشخص شده و میزان سازگاری محاسبه شده است. از نتایج فوق بهترین فیچری که هم در برابر تغییرات گوناگون مقاوم و تکرارپذیر باشد و هم دقت تشخیص و تفکیک‌پذیری مناسبی داشته باشد انتخاب خواهد شد و با مقایسه با فیچر کرتوسیس مشاهده شد که این فیچر وضعیت مناسبی در مقایسه با دیگر فیچرهای آماری از جمله هارمیان و مدیان ندارد.